Communication in Physical Sciences, 2026, 13(5):763-773

Defect-Dominated Performance Limits in $FASnI_3$ Perovskite Solar Cells: A Thickness-Dependent Simulation Study

Ejikeme Ezo Igbokwe, Elizabeth Chinyere Nwaokorongwu, Anthony Kalu Uchechukwu, Eke Chukwu Emole

Received: 06 January 2026/Accepted: 02 May 2026 /Published: 14 May 2026
https://dx.doi.org/10.4314/cps.v13i5.7

Abstract: *The performance of lead-free tin-based perovskite solar cells remains fundamentally constrained by defect-induced recombination losses, limiting their competitiveness with lead-based counterparts. In this work, a physically calibrated numerical investigation of an inverted (p–i–n) $FASnI_3$ perovskite solar cell is performed using the SCAPS-1D simulation framework. The model incorporates experimentally consistent material parameters, including bulk and interface defect states, as well as series and shunt resistive losses, enabling realistic reproduction of non-ideal device behaviour. A baseline power conversion efficiency of 14.02% is achieved, with an open-circuit voltage of 1.073 V, short-circuit current density of 27.48 mA/cm², and fill factor of 47.56%. A systematic thickness-dependent analysis (100–1000 nm) reveals a counterintuitive decline in device performance with increasing absorber thickness. While optical absorption improves marginally, enhanced Shockley–Read–Hall recombination and transport limitations dominate, leading to reduced carrier collection efficiency. Notably, the open-circuit voltage remains largely invariant, indicating a recombination-limited regime, whereas both current density and fill factor degrade with thickness. The optimal absorber thickness is identified within the range of 100–300 nm, where the balance between photogeneration and recombination losses is maximized. These findings demonstrate that device performance in $FASnI_3$ solar cells is fundamentally governed by carrier preservation rather than photon absorption. The study establishes a physically grounded framework for thickness optimization and highlights the critical role of defect passivation and interface engineering in advancing high-efficiency, lead-free perovskite solar cells.*

Keywords: *$FASnI_3$, lead-free perovskites, SCAPS-1D, SRH recombination, thickness optimization, charge transport, defect states*

Ejikeme Ezo Igbokwe*
Department of Physics with Electronics, Ogbonnaya Onu Polytechnic, Aba (formerly Abia State Polytechnic, Aba).
Email: ejikeme.igbokwe@abiastatepolytechnic.edu.ng;
https://orcid.org/0000-0003-1834-8614

Elizabeth Chinyere Nwaokorongwu
Department of Physics, Michael Okpara University of Agriculture.
Email: nwaokorongwu.elizabeth@mouau.edu.ng

Anthony Kalu Uchechukwu
Department of Physics with Electronics, Ogbonnaya Onu Polytechnic, Aba (formerly Abia State Polytechnic, Aba).
Email: anthony.uchechukwu@abiastatepolytechnic.edu.ng

Eke Chukwu Emole
Department of Chemistry/Biochemistry, Ogbonnaya Onu Polytechnic, Aba (formerly Abia State Polytechnic, Aba).
Email : emole.eke@abiastatepolytechnic.edu.ng

1.0 Introduction

The accelerating global transition toward low-carbon and sustainable energy systems has intensified the demand for next-generation photovoltaic technologies capable of combining high efficiency, low production cost, and environmental sustainability."

Metal–halide perovskite solar cells (PSCs) have emerged as one of the most promising candidates, achieving certified power conversion efficiencies exceeding 26% in single-junction devices (National Renewable Energy Laboratory [NREL], 2024). This rapid progress has been largely driven by lead-based perovskites such as methylammonium and formamidinium lead

halides, which exhibit excellent optical absorption, long carrier diffusion lengths, and tunable electronic properties (Jeong *et al*., 2021; Min *et al*., 2021). Despite these advantages, the presence of toxic lead remains a major barrier to large-scale deployment, raising concerns related to environmental impact and long-term sustainability (Babayigit *et al*., 2021; Wang *et al*., 2019). As a result, considerable research attention has increasingly focused on the development of lead-free alternatives, among which tin-based perovskites have attracted considerable attention. In particular, formamidinium tin iodide ($FASnI_3$) is regarded as a leading candidate due to its near-ideal bandgap (~1.4 eV), which is well aligned with the Shockley–Queisser limit for single-junction solar cells (Jiang *et al*., 2019; Tai *et al*., 2019). In addition, $FASnI_3$ exhibits high absorption coefficients and favorable charge transport properties, making it suitable for efficient light harvesting. Despite continuous progress, the certified efficiencies of tin-based perovskite solar cells still remain substantially lower than those of lead-based analogues due to severe defect-assisted recombination losses. However, the practical performance of $FASnI_3$-based solar cells remains significantly lower than that of their lead-based counterparts. This limitation is primarily attributed to the intrinsic instability of Sn^{2+}, which readily oxidizes to Sn^{4+} under ambient conditions. The oxidation of Sn^{2+} to Sn^{4+} generates a high density of vacancy-related defect states and results in strong p-type self-doping, leading to increased non-radiative recombination losses (Shao *et al*., 2018; Ren *et al*., 2025). Under these defect-rich conditions, Shockley–Read–Hall (SRH) recombination becomes the dominant non-radiative carrier loss mechanism, severely limiting both the open-circuit voltage and fill factor (Wu *et al*., 2021). Consequently, improving device performance requires not only efficient light absorption but, more critically, effective suppression of recombination pathways.

Device architecture plays a crucial role in mitigating these losses. The inverted (p–i–n) configuration has emerged as a preferred structure for tin-based perovskite solar cells due to its reduced hysteresis, improved interfacial charge extraction, and compatibility with low-temperature fabrication processes (Li *et al*., 2023; Lin *et al*., 2019). Nevertheless, even within optimized architectures, device performance remains highly sensitive to both interfacial defect densities and geometric parameters, particularly the thickness of the absorber layer.

Absorber thickness is a key design parameter that governs the balance between optical generation and carrier recombination. In principle, increasing thickness enhances photon absorption and should lead to higher short-circuit current density. However, in defect-rich materials such as $FASnI_3$, thicker films also increases carrier transport distance, thereby enhancing the probability of recombination before charge collection. Although several studies have explored thickness optimization in perovskite solar cells, most analyses rely on idealized assumptions and do not adequately capture the recombination-dominated regime characteristic of tin-based systems (Decock *et al*., 2011). As a result, the fundamental relationship between thickness, carrier transport, and recombination losses remains insufficiently understood. To date, limited studies have systematically examined the interplay between absorber thickness and defect-mediated recombination under physically realistic operating conditions in inverted $FASnI_3$ solar cells.

Numerical simulation offers a powerful approach for isolating and analyzing these competing mechanisms. Numerical tools such as SCAPS-1D enable self-consistent solution of the coupled Poisson and continuity equations governing charge transport, recombination, and electrostatic behavior within photovoltaic devices (Burgelman *et al*., 2013). However, the reliability of such simulations critically depends on physical calibration.Simulation models that neglect bulk defects, interface recombination, and parasitic resistive effects frequently predict unrealistically high efficiencies that are inconsistent with experimentally achievable device performance."

In this study, a physically calibrated SCAPS-1D model of an inverted $FASnI_3$ perovskite solar cell is developed to investigate thickness-dependent performance under realistic conditions. Unlike previous studies that assume ideal transport, the present work explicitly incorporates bulk and interface defect states, as well as resistive losses, to capture the recombination-limited nature of tin-

based devices. By systematically varying the absorber thickness from 100 nm to 1000 nm while maintaining all other parameters constant, the study isolates the intrinsic impact of thickness on device performance.

Unlike idealized simulations reported in previous studies, the present model incorporates experimentally relevant defect-assisted recombination and parasitic resistive losses. To date, limited studies have systematically examined the interplay between absorber thickness and defect-mediated recombination under physically realistic operating conditions in inverted $FASnI_3$ solar cells. The primary objective of this work is to establish a physically grounded understanding of the competing relationship between optical absorption enhancement and defect-assisted carrier recombination as a function of absorber thickness. The findings provide physically meaningful design guidelines for optimizing absorber geometry, defect passivation strategies, and interfacial engineering toward the realization of high-efficiency and environmentally benign lead-free perovskite solar cells.

1.0 Materials and Methods

2.1 Numerical Simulation Framework

Numerical device simulations were performed using SCAPS-1D, a widely validated one-dimensional semiconductor simulation tool for modelling thin-film photovoltaic devices. SCAPS solves the coupled Poisson and continuity equations for electrons and holes under steady-state conditions, enabling self-consistent evaluation of electrostatic potential, carrier transport, and recombination processes within multilayer semiconductor structures (Burgelman *et al*., 2013). The simulations were based on the self-consistent numerical solution of Poisson's equation together with the electron and hole continuity equations under steady-state conditions. Carrier transport was governed by drift–diffusion mechanisms, while recombination processes were modelled using the Shockley–Read–Hall formalism.

All simulations were conducted under standard test conditions: AM1.5G illumination (1000 W m^{-2}), temperature of 300 K, and "spatially distributed optical generation within the absorber layer based on the AM1.5G solar spectrum. . The simulator outputs included current density–voltage (J–V) characteristics, external quantum efficiency (EQE), and spatial recombination profiles.

To ensure numerical stability and physical consistency, thermionic emission boundary conditions implemented within SCAPS were applied, with ohmic contacts assumed at both electrodes. The front contact (FTO) and back contact (Ag) were defined with work functions aligned to facilitate efficient carrier extraction.

2.2 Device Architecture and Layer Configuration

The device investigated in this work follows an inverted (p–i–n) architecture, selected because of its experimentally demonstrated advantages in tin-based perovskite systems, including reduced hysteresis and improved operational stability.

The simulated structure is defined as:

(i) Front Contact: Fluorine-doped tin oxide (FTO)
(ii) Hole Transport Layer (HTL): PEDOT:PSS (40 nm)
(iii) Absorber Layer: $FASnI_3$ (variable thickness: 100–1000 nm)
(iv) Electron Transport Layer (ETL): PCBM (50 nm)
(v) Back Contact: Silver (Ag)

This configuration is illustrated in Fig. 1, which shows the energy band alignment and layer stacking of the device.

The choice of PEDOT:PSS and PCBM is not arbitrary; both materials are widely used in inverted perovskite solar cells due to their favourable energy alignment with $FASnI_3$ and their ability to facilitate efficient hole and electron extraction, respectively.The energy level alignment between PEDOT:PSS, $FASnI_3$, and PCBM promotes efficient charge separation while suppressing interfacial carrier accumulation. More importantly, this architecture minimizes interfacial energy barriers, which is critical for reducing recombination losses in tin-based systems.

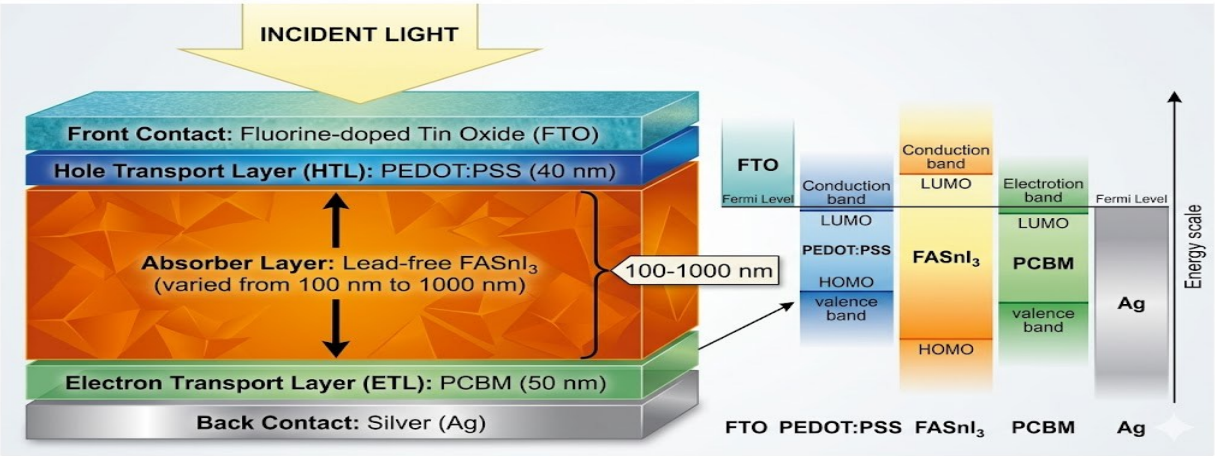

Fig. 1. Schematic illustration of the inverted (p–i–n) $FASnI_3$ perovskite solar cell architecture and corresponding equilibrium energy band diagram

2.3 Physical and Recombination Parameters

The optoelectronic properties of each layer were selected based on experimentally reported values for inverted perovskite solar cells. Table 1 summarizes the primary optoelectronic properties of each layer, including bandgap (E_g), electron affinity (χ), and carrier mobilities (μ). "Special consideration was given to the $FASnI_3$ absorber layer , where an acceptor density of 10^{16} cm^{-3} was used to reflect the intrinsic p-type self-doping behaviour experimentally associated with Sn vacancy formation and Sn^{2+} oxidation. All material parameters were adopted from experimentally reported and previously validated literature values for tin-based inverted perovskite solar cells.

Table 1: Main Physical Parameters Used for the Baseline Inverted (p-i-n) $FASnI_3$ Device Simulation

Parameter	PEDOT:PSS (HTL)	$FASnI_3$ (Absorber)	PCBM (ETL)
Thickness (d)	40 nm	500 nm	50 nm
Bandgap (Eg)	3.20 Ev	1.41 eV	2.00 Ev
Electron Affinity (χ)	2.20 Ev	4.17 eV	4.00 Ev
Dielectric Permittivity (ϵr)	3	8.2	3.9
CB DOS (Nc)	10^{19} cm^{-3}	10^{18} cm^{-3}	10^{18} cm^{-3}
VB DOS (Nv)	10^{19} cm^{-3}	10^{18} cm^{-3}	10^{18} cm^{-3}
Electron Mobility (μn)	10−3 cm^2/Vs	16 cm^2/Vs	$2\times10^{-3}cm^2/Vs$
Hole Mobility (μp)	10−3 cm^2/Vs	16 cm^2/Vs	$2\times10^{-3}cm^2/Vs$
Doping (N_A/N_D)	N_A:10^{18} cm^{-3}	N_A :10^{16} cm^{-3}	N_D :10^{18} cm^{-3}

2.4 Defect Physics and Recombination Model (Table 2)

Equal electron and hole mobilities were assumed for the absorber layer to simplify transport analysis and maintain consistency with experimentally reported balanced transport behaviour in $FASnI_3$ films. To capture non-ideal device behaviour, both bulk and interface defect states were incorporated explicitly. Defect-assisted Shockley–Read–

Hall (SRH) recombination was assumed \ to be the dominant recombination mechanism, consistent with experimental observations in tin-based perovskites (Shao *et al*., 2018; Wu *et al*., 2021). Bulk defects were introduced within the $FASnI_3$ absorber, while interface defects were defined at the $FASnI_3$/PCBM junction. Interface recombination was assigned a higher defect density and capture cross-section, reflecting experimentally observed interfacial recombination dominance in tin-based perovskite devices.
Series resistance (Rs) and shunt resistance (Rsh) were also included to account for resistive losses and leakage currents, respectively. These parameters are critical for accurately reproducing the fill factor and overall J–V characteristics.

Table 2: Defect and Resistance Parameters (Recombination Model)

Parameter	Bulk ($FASnI_3$)	Interface ($FASnI_3$ /PCBM)
Defect Type	Neutral	Neutral
Energy Distribution	Single	Single
Energy Level (Et)	0.6 eV (Above Ev)	0.6 eV (Above Ev)
Defect Density (Nt / Nit)	10^{11} cm^{-3}*	10^{14} cm^{-2}
Capture Cross-section (σn,p)	10^{-15} cm^2	10^{-13} cm2
Series Resistance (Rs)	---	20 Ω·cm^2
Shunt Resistance (Rsh)	---	1000 Ω·cm^2

2.5 Thickness Optimization Strategy

The selected trap energy level positioned above the valence band represents deep defect states capable of facilitating efficient non-radiative carrier recombination. To isolate the intrinsic effect of absorber thickness, the thickness of the $FASnI_3$ layer was systematically varied from 100 nm to 1000 nm, while all other parameters were held constant. The selected thickness range encompasses ultrathin to relatively thick absorber layers commonly investigated in experimental tin-based perovskite fabrication. This approach ensures that "…observed performance variations can be directly attributed to thickness-dependent changes For each thickness value, the following device characteristics were extracted:

(i) Current density–voltage (J–V) response
(ii) Open-circuit voltage (Voc)
(iii) Short-circuit current density (Jsc)
(iv) Fill factor (FF)
(v) Power conversion efficiency (PCE)
(vi) External quantum efficiency (EQE)
(vii) Recombination rate profiles

Radiative and Auger recombination mechanisms were neglected in the present model because SRH recombination is widely recognized as the dominant carrier loss pathway in defect-rich tin-based perovskite systems.

1.1 Methodological Framework

The overall methodology follows three sequential stages, namely

(i) Device Construction: Definition of a realistic inverted $FASnI_3$ solar cell architecture
(ii) Physical Calibration: Incorporation of experimentally consistent material and defect parameters
(iii) Parametric Analysis: Systematic variation of absorber thickness to evaluate performance trade-offs

This structured approach ensures that the simulation results reflect physically meaningful device behaviour and provide reliable guidance for practical device optimization.

3.0 Results and Discussion

3.1 Device Physics Governing the Baseline J–V Characteristics

The simulated current density–voltage (J–V) characteristics of the calibrated device (Fig. 2) yield a power conversion efficiency (PCE) of

14.02%, with an open-circuit voltage (V_oc) of 1.073 V, short-circuit current density (J_sc) of 27.48 mA cm^{-2}, and fill factor (FF) of 47.56%. While the relatively high V_oc and J_sc indicate efficient photogeneration and favorable band alignment, the suppressed FF reflects pronounced non-ideal losses.

The device behaviour can be described by the non-ideal diode equation:

$$J = J_{ph} - J_0\left[\exp\left(\frac{q(V+JR_s)}{nkT}\right) - 1\right] - \frac{V+JR_s}{R_{sh}} \quad (1)$$

where $J_0$is the saturation current density, n is the ideality factor, and Rs and R_{sh} represent series and shunt resistances, respectively. The reduced FF indicates substantial non-idealities arising from combined series resistance losses and enhanced recombination near the maximum power point. from both recombination currents (high J_0) and resistive losses, which distort the J–V curve near the maximum power point. This behaviour is consistent with experimentally reported $FASnI_3$ devices, where defect-assisted recombination dominates carrier dynamics (Shao *et al*., 2018; Wu *et al*., 2021).

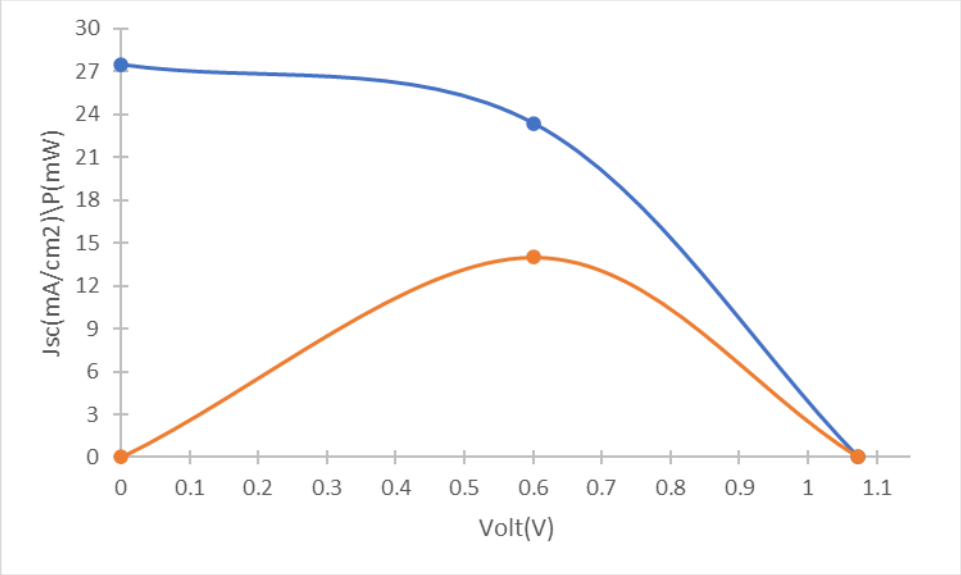

Fig. 2. Simulated current density–voltage (J–V) characteristics of the baseline $FASnI_3$ solar cell under AM1.5G illumination.

3.2 Recombination Physics and Voltage Limitation

The variation of Voc with absorber thickness (Fig. 3) shows minimal dependence on thickness, indicating that the device operates in a recombination-limited regime. The open-circuit voltage is governed by the quasi-Fermi level splitting and can be expressed as:

$$V_{oc} = \frac{kT}{q}\ln\left(\frac{J_{sc}}{J_0} + 1\right) \quad (2)$$

Since J_{sc} varies only weakly with thickness and the recombination current J0J_0J0 remains dominated by defect states, the ratio J_{sc}/J_0 remains nearly constant. As a result, V_oc exhibits negligible variation across the thickness range.

The dominant recombination pathway is Shockley–Read–Hall (SRH) recombination, given by:

$$R_{SRH} = \frac{np - n_i^2}{\tau_p(n+n_1)+\tau_n(p+p_1)} \quad (3)$$

Where τ_n and τ_p are carrier lifetimes determined by defect density and capture cross-sections. In $FASnI_3$, the high density of intrinsic defects reduces carrier lifetimes, thereby increasing recombination rates and limiting quasi-Fermi level splitting. Consequently, Voc becomes insensitive to geometric parameters such as thickness, as confirmed by the simulation results.

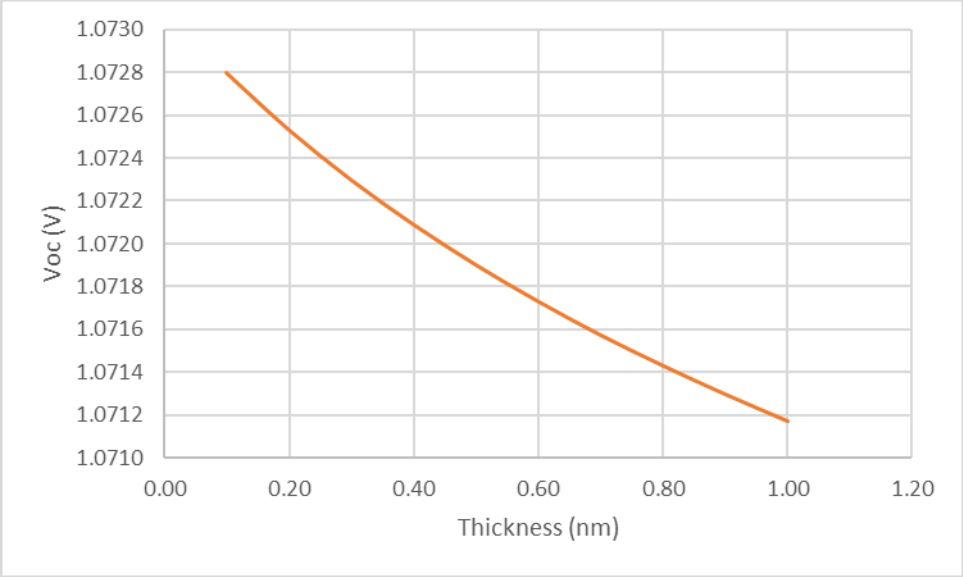

Fig. 3. Variation of open-circuit voltage (V_oc) as a function of absorber thickness (100–1000 nm).

3.3 Thickness-Dependent Carrier Collection and Current Loss

Contrary to the expectation that thicker absorbers enhance photocurrent, the simulated J_sc decreases slightly with increasing thickness (Fig. 4). This behaviour reflects a transition from an absorption-limited to a transport-limited regime.

Carrier collection is governed by the diffusion length:

$$L = \sqrt{D\tau} \quad (4)$$

where D is the diffusion coefficient and τ is the carrier lifetime. When the absorber thickness d exceeds L, photogenerated carriers recombine before reaching the charge-selective contacts. Under these conditions, the collection efficiency decreases with depth, leading to a reduction in J_{sc}. The current density can therefore be expressed as:

$$J_{sc} \int_0^d G(x)\,,\eta_c(x),dx \quad 5 \quad (5)$$

where G(x) is the generation rate and $\eta_c(x)$ is the position-dependent collection efficiency. In defect-rich $FASnI_3$, $\eta_c(x)$ decreases rapidly with depth due to SRH recombination, offsetting the marginal gains in optical absorption at larger thicknesses. This explains the observed decline in J_{sc} with increasing absorber thickness.

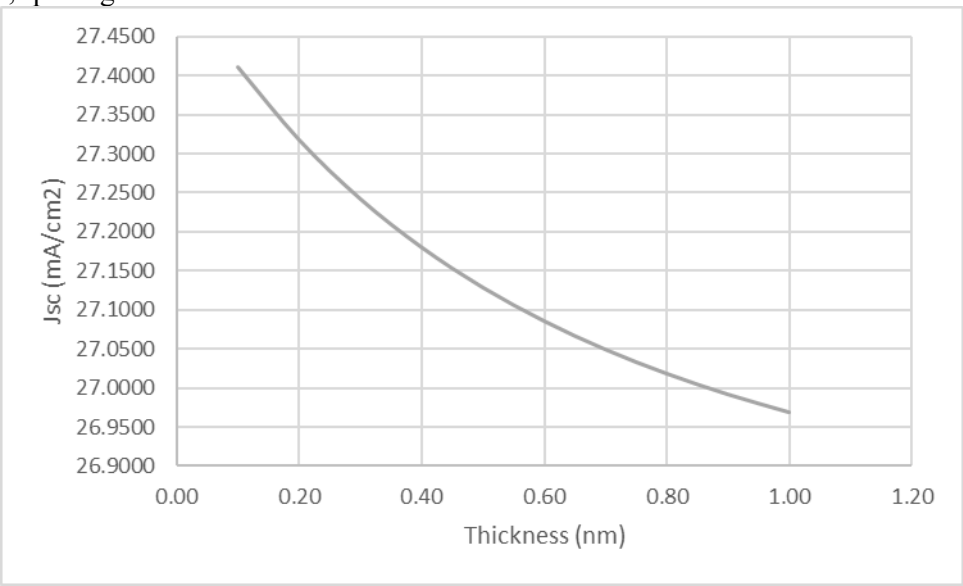

Fig. 4. Dependence of short-circuit current density (J_sc) on absorber thickness.

3.3 Fill Factor Degradation: Resistive and
3.3.1 Recombination Coupling

The fill factor exhibits a monotonic decrease with thickness (Fig. 5), with a more pronounced drop

at thicknesses above ~800 nm. This behaviour arises from the coupled effects of increased series resistance and enhanced recombination under forward bias.

As the absorber thickness increases, the average carrier transit distance becomes larger, leading to higher resistive losses and reduced electric field strength. Simultaneously, recombination currents increase, flattening the J–V curve near the maximum power point. The FF is therefore particularly sensitive to both transport limitations and recombination kinetics.

This coupling can be qualitatively understood from Eq. (1), where both R_s and J_0 influence the curvature of the J–V characteristics. In thick absorbers, the simultaneous increase in these loss mechanisms leads to a compounded reduction in FF, consistent with experimental observations in tin-based perovskite solar cells (Wang *et al*., 2019; Lin *et al*., 2019).

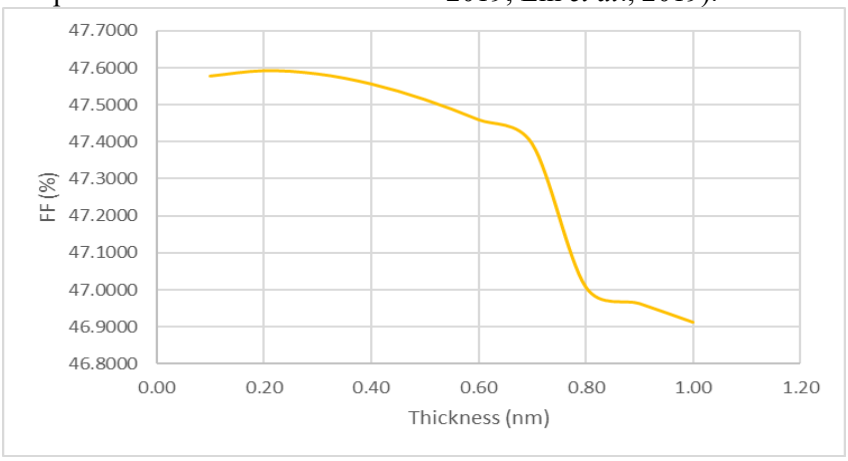

Fig. 5. Fill factor (FF) variation with absorber thickness

3.3.2 Efficiency Trade-Off and Optimal Thickness

The overall efficiency follows the relation:

$$\eta = \frac{V_{oc} \cdot J_{sc} \cdot FF}{P_{in}} \quad (6)$$

Given the near-constant V_oc, the variation in efficiency is primarily governed by J_sc and FF. The results show a gradual decline in PCE from ~13.99% at 100 nm to ~13.55% at 1000 nm (Fig. 6).

This trend reflects a fundamental trade-off between optical absorption and electrical losses. While thicker absorbers marginally increase photon absorption, they also exacerbate recombination and resistive losses. The optimal thickness corresponds to the regime where the incremental gain in absorption is balanced by minimal recombination losses, which occurs in the range of 100–300 nm.

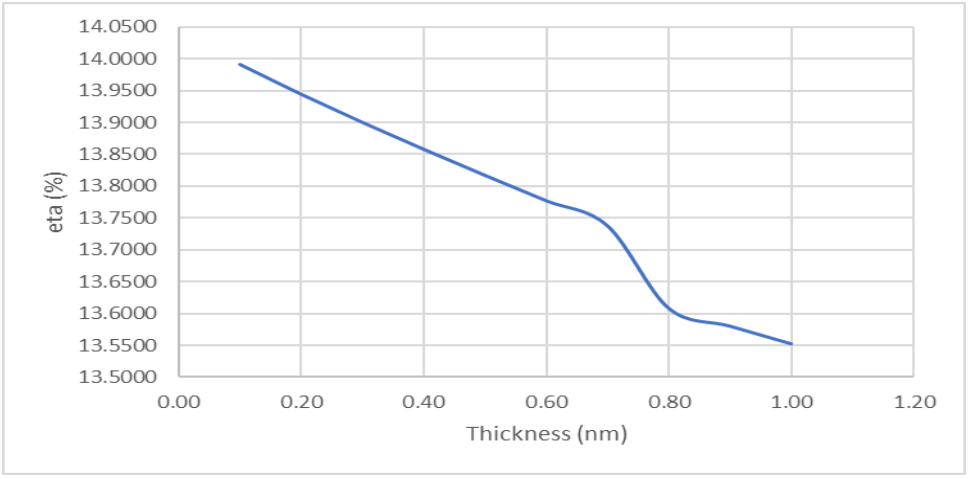

Fig. 6. Power conversion efficiency (PCE) as a function of absorber thickness

3.4 Recombination Dynamics and Physical Interpretation

The recombination profiles (Fig. 7) provide direct insight into the underlying loss mechanisms. The total recombination rate increases with thickness, confirming that thicker films introduce a larger recombination volume.

Two dominant recombination pathways are identified:

(i) Bulk SRH recombination, driven by intrinsic defects in $FASnI_3$

(ii) Interface recombination, particularly at the $FASnI_3$/PCBM junction

The increase in recombination with thickness explains all observed device trends:

(i) Constant V_oc: recombination already dominates and saturates voltage

(ii) Decreasing J_sc: increased carrier loss during transport

(iii) Reduced FF: enhanced recombination and resistive losses

(iv) Lower PCE: cumulative effect of all loss mechanisms

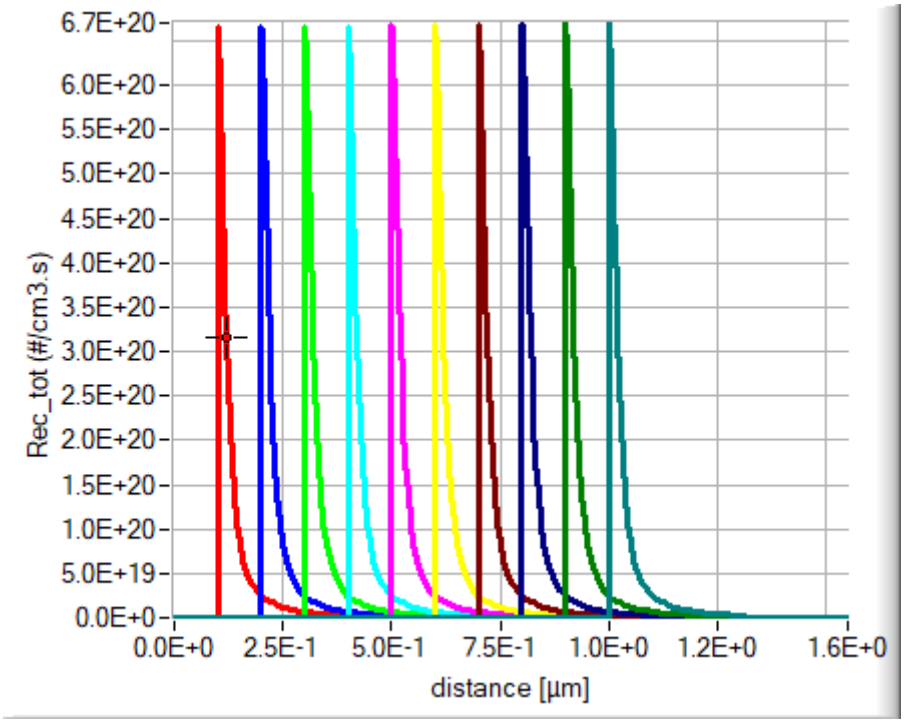

Fig. 8. Thickness-dependent recombination rate profile within the $FASnI_3$ absorber layer.

3.5 Unified Physical Interpretation

Across all performance metrics, a consistent physical picture emerges: Across all simulated thicknesses, device operation is consistently governed by a recombination-limited transport regime… . In this regime, increasing absorber thickness does not improve performance because carrier preservation—not photon absorption—becomes the limiting factor.

This finding challenges the conventional assumption that thicker absorbers inherently lead to higher efficiency and instead highlights the critical importance of controlling defect density and interface quality. Similar recombination-dominated behaviour has been reported in recent studies on tin-based perovskite solar cells, where efficiency improvements are primarily achieved through defect passivation and interface

engineering rather than geometric scaling (Tai *et al*., 2019; Ren *et al*., 2025).

3.6 Design Implications for High-Performance $FASnI_3$ PSCs

The results provide clear design guidelines for optimizing $FASnI_3$ solar cells. Efficient charge collection can be achieved by maintaining the absorber thickness within the carrier diffusion length. Reducing bulk defect density is essential for enhancing carrier lifetime and suppressing Shockley–Read–Hall (SRH) recombination, while engineering high-quality interfaces helps minimize interfacial recombination losses. In addition, improving carrier mobility reduces transport-related resistive losses. These strategies directly address the dominant loss mechanisms identified in this study and are crucial for improving the performance of lead-free perovskite solar cells. The findings further demonstrate that in defect-dominated perovskite systems, geometric optimization alone is insufficient to achieve significant performance enhancement without

simultaneous defect and interface engineering.

4.0 Conclusion

This work presents a physically calibrated numerical investigation of an inverted (p–i–n) $FASnI_3$ perovskite solar cellm with particular emphasis on the influence of absorber layer thickness on device performance.By incorporating realistic material parameters, defect states, and resistive losses, the model captures the non-ideal behaviour characteristic of tin-based perovskite devices.

The results demonstrate that device performance is primarily limited by defect-assisted recombination rather than optical absorption. Although increasing absorber thickness enhances light harvesting, it simultaneously increases carrier transport distance and recombination probability, leading to a measurable decline in short-circuit current density and fill factor. In contrast, the open-circuit voltage remains largely insensitive to thickness, confirming that the device operates in a recombination-limited regime.

An optimal thickness range of approximately 100–300 nm is identified, where the balance between photogeneration and carrier extraction is most favourable. Beyond this regime, recombination losses dominate, resulting in reduced overall efficiency. These findings establish that, for $FASnI_3$-based solar cells, performance optimization must prioritize carrier preservation over increased optical absorption.

From a device engineering perspective, the results highlight three critical pathways for performance enhancement: reduction of bulk and interface defect densities, improvement of charge transport through enhanced carrier mobility, and optimization of interfacial energy alignment to suppress recombination losses. Addressing these factors is essential for bridging the performance gap between tin-based and lead-based perovskite solar cells.

Future work should extend this analysis by coupling thickness optimization with defect density and interface engineering studies, as well as by validating simulation predictions against experimental device performance. Such integrated approaches are necessary to advance the practical realization of high-efficiency, environmentally sustainable, lead-free perovskite solar cells.

5.0 References

Babayigit, A., Duy Thanh, D., Ethirajan, A., Manca, J., Muller, M., Boyen, H.G. & Conings, B. (2016). Assessing the toxicity of Pb-and Sn-based perovskite solar cells in model organism Danio rerio. *Scientific reports*, *6, 1,* 18721, doi: 10.1038/srep18721

Burgelman, M., Decock, K., Khelifi, S., & Abass, A. (2013). Advanced electrical simulation of thin film solar cells. *Thin Solid Films*, 535, pp. 296-301. https://doi.org/10.1016/j.tsf.2012.10.032

Decock, K., Khelifi, S., & Burgelman, M. (2011). Modelling multivalent defects in thin film solar cells. *Thin Solid Films*, 519, 21, pp. 7481-7484.

Jeong, M., Choi, I. W., Go, E. M., Cho, Y., Kim, M., Lee, B., & Park, N. G. (2021). Pseudo-halide anion engineering for α-$FAPbI_3$ perovskite solar cells. *Nature*, 592, 7854, pp. 381–385.

Jiang, Q., Zhao, Y., Zhang, X., Yang, X., Chen, Y., Chu, Z., & You, J. (2019). Surface passivation of perovskite film for efficient solar cells. *Nature Photonics*, 13, 7, pp. 460–466.

Li, T., He, F., Liang, J. W., & Qi, Y. (2023). Functional layers in efficient and stable inverted tin-based perovskite solar cells. *Joule*, 7, 8, pp. 1731–1764.

Lin, R., Xiao, K., Qin, Z., Han, Q., Zhang, C., Wei, M., Saidaminov, M.I., Gao, Y., Xu, J., Xiao, M. & Li, A. (2019). Monolithic all-perovskite tandem solar cells with 24.8% efficiency exploiting comproportionation to suppress Sn (ii) oxidation in precursor ink. *Nature Energy*, *4, 10, pp.* pp.864-873.

Min, H., Lee, D.Y., Kim, J., Kim, G., Lee, K.S., Kim, J., Paik, M.J., Kim, Y.K., Kim, K.S., Kim, M.G. & Shin, T.J. (2021). Perovskite solar cells with atomically coherent interlayers on SnO2 electrodes. *Nature*, *598,* 7881, pp. 444-450.

National Renewable Energy Laboratory (NREL), (2024). *Best research-cell efficiencies*. ttps://www.nrel.gov/pv/cell-efficiency.html.

Ren, X., Wang, S., Lyu, W., Cai, H., Lyu, X., Gao, X., Lu, X., Wu, S. & Liu, J.M. (2025). Enhancing the Stability and Efficiency of Tin-Based Perovskite Solar Cells via Bifunctional Additive-Engineered Defect Passivation. *ACS Applied Materials & Interfaces*, 17, 21, pp/ .31051-31063.

Shao, S., Liu, J., Portale, G., Fang, H.H., Blake, G.R., ten Brink, G.H., Koster, L.J.A. & Loi, M.A. (2018). Highly reproducible Sn-based hybrid perovskite solar cells with 9% efficiency. *Advanced Energy Materials*, *8, 4,,* 1702019m **https://doi.org/10.1002/aenm.201702019Digital Object Identifier (DOI)**

Tai, Q., Guo, X., Tang, G., You, P., Ng, T.W., Shen, D., Cao, J., Liu, C.K., Wang, N., Zhu, Y. & Lee, C.S. (2019). Antioxidant grain passivation for air-stable tin-based perovskite solar cells. *Angewandte Chemie International Edition*, *58*(3), pp.806-810.

Wang, Y., Dar, M.I., Ono, L.K., Zhang, T., Kan, M., Li, Y., Zhang, L., Wang, X., Yang, Y., Gao, X. and Qi, Y. (2019). Thermodynamically stabilized β-CsPbI3–based perovskite solar cells with efficiencies> 18%. *Science*, *365,* 6453, pp.591-595.

Wu, T., Liu, X., Luo, X., Lin, X., Cui, D., Wang, Y., Segawa, H., Zhang, Y. & Han, L. (2021). Lead-free tin perovskite solar cells. *Joule*, *5, 4,* pp. 863-886.

Declaration

Consent for publication

Not applicable

Availability of data

Data shall be made available on demand.

Competing interests

The authors declared no conflict-of-interest

Ethical Consideration

Not applicable

Funding

The authors declared no external source of funding

Authors' contributions

Ejikeme Ezo Igbokwe conceived the study, performed SCAPS-1D simulations, analyzed data, and drafted the manuscript. Elizabeth Chinyere Nwaokorongwu contributed to device modeling, interpretation of photovoltaic parameters, and manuscript revision. Anthony Kalu Uchechukwu assisted in simulation validation, literature review, and data presentation. Eke Chukwu Emole contributed to theoretical analysis, result interpretation, proofreading, and final approval of the manuscript.